Mechanisms of Ligand Substitution Reactions in Ternary Dioxouranium(VI) Complexes

Zoltán Szabó and Ingmar Grenthe*

Department of Chemistry, Inorganic Chemistry, Royal Institute of Technology, (KTH), S-10044 Stockholm, Sweden

Received April 16, 1998

The activation parameters of various inter- and intramolecular ligand exchange reactions in ternary complexes of the type UO_2LF_3 (where L is one of the bidentate ligands picolinate, 4-nitropicolinate, 4-(3-pentyl)picolinate, oxalate, or carbonate) and UO_2L_2F (where L = picolinate or oxalate) have been determined by different NMR techniques. The activation entropies for the reactions have been used to discuss their intimate mechanism, particularly the solvent participation. Additional mechanistic information has been obtained from studies of H^+/D^+ catalysis of the various reactions. Through the use of the proton-catalyzed pathway, the rate of carbonate exchange in $UO_2CO_3F_3^{3-}$ was varied by a factor of ca. 10. The fact that the rate of fluoride exchange remained constant clearly indicates that the exchanges of carbonate and fluoride follow parallel pathways. The activation entropies of most of the fluoride exchange reactions in UO_2LF_3 have values close to 10 J K^{-1} mol^{-1}, indicating dissociative (D) or dissociative interchange (I_D) mechanisms. The exchange of L takes place in two steps: The first is a chelate ring opening/closing, resulting in a ligand rotation. The second is bond breaking at the carboxylate end and exchange; hence, the activation entropies for the exchange vary with L. In the 4-nitropicolinate and carbonate systems, where the exchange of L is faster than that of F^-, the exchange takes place in a dissociative reaction via the intermediate/transition state "UO_2F_3", which contains a lower number of coordinated water molecules than that of $UO_2(H_2O)_2F_3^-$. There is no evidence of the presence of unidentate L at equilibrium, indicating that the equilibrium constant for the ring opening, $K = k_1/k_{-1}$, is smaller than 0.05. Hence, the observed rate constant for the ligand rotation is approximately equal to that for the ring opening whereas that of the ring closing is at least 20 times larger. The activation entropies for these reactions indicate a much smaller involvement of water in the activated state in the 4-nitropicolinate complex than those of the other two picolinates, a signature of reactions of I_D mechanisms. The exchange of fluoride and oxalate in $UO_2(oxalate)_2F^{3-}$ is first-order with respect to the concentration of the complex and independent of the concentrations of free fluoride and oxalate. The fact that the exchange of oxalate is independent of the free oxalate concentration but still slower than that of fluoride shows that they take place along separate pathways and not as consecutive reactions along the fluoride exchange pathway. The exchange reactions have nearly the same activation parameters whereas those for the fluoride exchange change significantly between H_2O and D_2O. This together with the negative activation entropy, −74 J K^{-1} mol^{-1}, indicates solvent participation in the activated state, presumably an I_D mechanism with extensive solvation of the leaving fluoride. All ligand exchange reactions are proton-catalyzed with a reverse-isotope effect, indicating the formation of a protonated precursor. The exchange reactions also are catalyzed to a small extent by hydrofluoric and acetic acids, which act as proton donors, without the involvement of the conjugate bases in the exchange reactions. These reactions have normal isotope effects.

Introduction

In two previous papers, we have discussed the structure, isomerism, and ligand dynamics in the binary[1] and ternary dioxouranium(VI) complexes[2] UO_2LF_n ($n = 1-3$) and UO_2L_2F (L = oxalate (ox), picolinate (pic), carbonate, or acetate (ac) in aqueous solution). All exchange reactions in the binary UO_2^{2+}−fluoride system followed second-order rate laws involving the different complexes and F^-/HF as reactants. We suggested for most of them an I_D (concerted) mechanism of the Eigen−Wilkins type, involving bond breaking of a leaving water and bond formation of the entering nucleophile in the rate-determining step. The rate of ligand exchange in the binary systems was too fast to allow the identification of different stereoisomers, e.g., the two possible isomers of $UO_2(H_2O)_2F_3^-$. The rates of exchange in the ternary complexes are much smaller, and we were able to identify both inter- and intramolecular exchange pathways. Both were first-order with respect to the concentration of the complex studied and were independent of the concentration of the exchanging ligand. The rate of exchange of coordinated fluoride was approximately independent of L whereas that for the exchange of L was very near the same, but it was 2−3 times slower than that of fluoride, with the exception of acetate and 4-nitropicolinate. These findings may indicate either D or I_D mechanisms. However, A or I_A mechanisms also are possible if the water solvent participates in the exchange reactions.

The mechanisms for intra- and intermolecular exchange reactions have previously been studied in different noncoordinating, or weakly coordinating solvents. Kramer et al.[3] studied the dynamics of complexes of uranyl hexafluoroacetylacetonate

* To whom correspondence should be addressed. Fax: 46-8-212626. E-mail: ingmarg@inorg.kth.se.

(1) Szabó, Z.; Glaser, J.; Grenthe, I. *Inorg. Chem.* **1996**, *35*, 2036.
(2) Szabó, Z.; Aas, W.; Grenthe, I. *Inorg. Chem.* **1997**, *36*, 5369.
(3) Kramer, G. M.; Dines, M. B.; Kastrup, R.; Melchior, M. T.; Maas, E. T., Jr. *Inorg. Chem.* **1981**, *20*, 3.

10.1021/ic9804364 CCC: $15.00
Published on Web 11/06/1998

with different Lewis bases using ^{19}F NMR spectroscopy and interpreted the fluxionality of the coordinated hexafluoroacetylacetonate as a result of a migration of the Lewis base "over a restricted potential energy surface from one side of the uranyl ion to the other". Glavincevski and Brownstein[4] studied similar reactions for other adducts and concluded that the rotation of the β-diketone ring is a result of the fluxionality in the adducts. They discarded the base migration hypothesis of Kramer[3] on stereochemical grounds. Fukutomi et al.[5−7] studied inter- and intramolecular exchange reactions of the ternary β-diketonate complexes $UO_2(\beta\text{-diketonate})_2L$ (where L is a Lewis base such as dimethyl sulfoxide, *N*,*N*-dimethylformamide, or *N*,*N*-diethylformamide) and discussed different mechanistic schemes involving both dissociative and interchange pathways. These studies are relevant for the mechanistic discussions of exchange reactions in the $UO_2(ox)_2F^{3-}$ complex. Studies of intermolecular ligand exchange in $UO_2(NIPA)_3$ (where NIPA is nonamethylimidophosphoramide) have been made by Delpuech et al.,[8,9] who suggest that the reactions take place via a chelate ring opening, followed by "internally assisted ligand displacement, quite analogous to an internal nucleophilic substitution about a saturated carbon atom".

There are important differences between these exchange reactions and those studied in our previous communication,[1] for example, the much larger differences among the rates of exchange of the bidentate ligand and the different Lewis bases in the nonaqueous systems and those between L and fluoride in water. Dissociative pathways are more probable in noncoordinating solvents than in aqueous systems. These differences may be exploited to obtain better understanding of the mechanisms for the various exchange reactions. In particular, we want to explore (1) whether the ligand exchange reactions follow parallel or consecutive pathways and (2) the intimate mechanisms of the intra- and intermolecular exchange reactions, to decide if they are associatively or dissociatively activated.

To achieve this, we expanded studies of the reactions in our previous paper (viz., determinations of the activation parameters for the reactions) and investigated proton-catalyzed pathways, including those with H/D isotope effects.

Experimental Section

Chemicals and Solutions. A uranium(VI) perchlorate stock solution was prepared as described earlier.[10] NaF, Na_2CO_3, $Na_2(C_2O_4)$, CH_3COONa, and picolinic, 4-nitropicolinic, and 4-(3-pentyl)picolinic acids were used to prepare the various test solutions. At lower total fluoride ion concentrations, the pH was measured and recalculated to concentrations, as described before.[1] Solutions of $HClO_4$ and NaOH were used to vary the hydrogen ion concentration. ^{13}C NMR measurements were made using solutions of ^{13}C-enriched $Na_2(C_2O_4)$ (Isotec, Inc., 99.2% ^{13}C) and Na_2CO_3 (Stohler Isotope Chemical, 99.3% ^{13}C).

NMR Measurements. The NMR spectra were recorded on a Bruker DMX500 spectrometer. D_2O solutions (5%) were used in the locked mode. The temperature control/measurement technique was the same as before;[1] however, the temperatures were checked and recalculated from the chemical shifts of methanol,[11] as well. The test solutions were measured in 5-mm (for ^{19}F and ^1H) or 10-mm (for ^{13}C) NMR tubes with Teflon inserts for the acid solutions. The ^{19}F NMR spectra recorded at 470.5 MHz were referenced to an aqueous solution of 0.01 M NaF in 1 M $NaClO_4$ (pH = 12) at 25 °C, and the ^{13}C NMR spectra (at 125.7 MHz) and the ^1H NMR spectra (at 500.1 MHz) were referenced to the methyl signal of sodium 3-(trimethylsilyl)propionate-d_4 at 25 °C. Selective inversion-transfer experiments were performed using Gaussian pulses.[12,13]

Data Treatment

Equilibrium Calculations. The experiments have been made in a 1.00 M $NaClO_4$ ionic medium using the equilibrium constants described in a recent paper.[14] The equilibrium distribution of the solutions was calculated and graphically presented using the MEDUSA program.[15] In solutions where the HF-resistant pH electrode could not be used ($[F^-]_{tot} > 50$ mM), the equilibrium proton concentration was calculated from the chemical shift of the exchange-averaged ^{19}F NMR signal of HF/F^- according to the formula

$$-\log [H^+] = pK_{HF} - \log[(\delta_{F^-} - \delta_{obs})/(\delta_{obs} - \delta_{HF})] \quad (1)$$

where δ_{obs} is the observed fluorine shift in the solutions and δ_{F^-} and δ_{HF} are the shifts of the fluoride and HF signal, respectively. The measured shift differences for the individual species [$\delta_{F^-} = 0$ ppm, $\delta_{HF} = -42.5$ ppm, $\delta_{F^-} = -2.8$ ppm (in D_2O), and $\delta_{DF} = -47.3$ ppm] were similar to the data published earlier.[16] The measured H^+ or D^+ concentrations at lower total fluoride concentrations and the values calculated from eq 1 (using $pK_{HF} = 2.95$ and $pK_{DF} = 3.25$) agreed within 0.03 units in log [H^+], or log [D^+].

Dynamic Calculations. The applications of different dynamic NMR methods are very well documented in the literature, and we have given a summary of the methods used here in our previous papers.[1,2,17] The proton catalyzed exchange processes for $UO_2(ox)F_3^{3-}$ and $UO_2(ox)_2F^{3-}$ complexes could be treated as two-site cases, where the complex is one site and the free fluoride or oxalate is the other. However, one-dimensional magnetization-transfer experiments, inverting the signals of both sites, offered higher precision in most cases for the calculated rate constants at −5 °C than those calculated from the line broadening.

Determination of Activation Parameters. The activation parameters for the different complexes were in general determined from data in a pH range (between 6 and 8) where proton-catalyzed pathways were negligible and the systems could be treated as two-site cases. Because of the very large chemical shift difference between the coordinated and the free fluoride, separate signals were observed even at higher temperatures, and the intermolecular fluoride exchange rate could be calculated from the line broadening of the free fluoride signal. In the picolinate systems, the peaks of the coordinated fluorides are affected by both the intramolecular rotation of the picolinate and the external fluoride exchange. Because of the coupling, they had to be treated as multisite exchanges. The rate constants and the theoretical line shapes were calculated by a special

(4) Glavincevski, B.; Brownstein, S. *Inorg. Chem.* **1983**, *22*, 221.
(5) Ikeda, Y.; Tomiyasu, H.; Fukutomi, H. *Inorg. Chem.* **1984**, *23*, 1356.
(6) Ikeda, Y.; Tomiyasu, H.; Fukutomi, H. *Inorg. Chem.* **1984**, *23*, 3197.
(7) Ikeda, Y.; Tomiyasu, H.; Fukutomi, H. *Bull. Chem. Soc. Jpn.* **1984**, *57*, 2925.
(8) Bokolo, K.; Delpuech, J.-J.; Rodehuser, L.; Rubini, P. R. *Inorg. Chem.* **1981**, *20*, 992.
(9) Rodehuser, L.; Rubini, P. R.; Bokolo, K.; Delpuech, J.-J. *Inorg. Chem.* **1982**, *21*, 1061.
(10) Ciavatta, L.; Ferri, D.; Grenthe, I.; Salvatore, F. *Inorg. Chem.* **1981**, *20*, 463.
(11) Geet, A. L. V. *Anal. Chem.* **1970**, *42*, 679.
(12) Kessler, H.; Mronga, S.; Gemecker, G. *Magn. Reson. Chem.* **1991**, *29*, 527.
(13) Freeman, R. *Chem. Rev.* **1991**, *91*, 1397.
(14) Aas, W.; Moukhamet-Galeev, A.; Grenthe, I. *Radiochim. Acta*, in press.
(15) Puigdomenech, I. *MEDUSA (Windows Interface to the MS-DOS Versions of INPUT, SED and PREDOM: Fortran Programs Drawing Chemical Equilibrium Diagrams)*; 1997.
(16) Schaumburg, K.; Deverell, C. *J. Am. Chem. Soc.* **1968**, *90*, 2495.
(17) Szabó, Z.; Glaser, J. *Magn. Reson. Chem.* **1995**, *33*, 20−26.

Table 1. Activation Parameters for the Exchange Reactions Studied

reaction	$\Delta H^{\ddagger}$ (kJ mol^{-1})	$\Delta S^{\ddagger}$ (J mol^{-1} K^{-1})	$k_{(obs)}$ (s^{-1})[a]
$UO_2CO_3F_3 \leftrightarrow$ F	53.7(1.6)[b]	−15.7(0.8)	14.2(2.1)
	52.5(1.7)[c]	−18.7(0.6)	15.9(1.8)
$UO_2(pic)F_3 \leftrightarrow$ F	61.4(1.6)	14.6(0.5)	24.4(0.6)[d,e]
			12.8(0.3)[e,f]
$UO_2(i\text{-pentyl-pic})F_3 \leftrightarrow$ F	59.7(1.2)	10.4(0.8)	18.2(1.8)[d]
			13.9(1.1)[f]
$UO_2(NO_2\text{-pic})F_3 \leftrightarrow$ F	60.3(2.6)	14.6(0.6)	16.0(1.2)
$UO_2(pic)F_3 \leftrightarrow$ pic	56.2(4.2)	−16.3(1.2)	4.7(0.2)[e]
$UO_2(NO_2\text{-pic})F_3 \leftrightarrow NO_2\text{-pic}$	59.4(1.4)	11.3(0.4)	55[g]
picolinate rotation	40.1(2.4)[h]	−46.7(2.8)	300
	46.8(1.5)[i]	−32.8(1.0)	90
	49.6(3.4)[j]	3.3(1.2)	2060
$UO_2(ox)F_3 \leftrightarrow$ F	58.9(3.4)	12.4(1.0)	21.6(2.4)[d,e]
	60.4(2.0)[k]	18.9(0.6)	14.1(0.8)[e,f]
$UO_2(ox)F_3 \leftrightarrow$ ox	70.2(5.6)	23.1(1.8)	6.2(0.2)[e]
$UO_2(pic)_2F \leftrightarrow$ F	34.6(1.4)	−97.8(4.0)	12.6(1.5)[e]
$UO_2(ox)_2F \leftrightarrow$ F	40.8(2.0)	−74.8(3.6)	12.3(1.0)[e]
	47.1(2.6)[k]	−56.3(3.2)	
$UO_2(ox)_2F \leftrightarrow$ ox	42.9(3.4)	−73.3(5.8)	8.7(1.5)[e]

[a] At −5 °C. [b] At pH = 8.5. [c] At pH = 7.1. [d] For the central fluoride. [e] Previously reported figures.[2] [f] For the edge fluorides. [g] Calculated using the activation parameters. [h] For picolinate. [i] For 4-(3-pentyl)picolinate. [j] For 4-nitropicolinate. [k] In D_2O.

MATLAB[18] program using the matrix formalism suggested in the literature.[19] The fairly small ^{13}C NMR shift difference between coordinated and free ligands (oxalate or carbonate) resulted in fast exchange when the temperature was increased; the line shape of the coalesced peaks was calculated by the same program from the individual chemical shifts and the relative populations of the exchanging species. The experimental line widths were determined by either fitting of a Lorentzian curve to the individual signals or a deconvolution of the overlapping peaks using the WIN-NMR program.[20] The relatively broad temperature region and the good accuracy of both the temperature measurements and the line width determination allowed us to evaluate the activation parameters with a high degree of precision. The errors given in Table 1 represent the uncertainties at the 2σ level in the linear regression analysis.

Results and Discussion

On the basis of the experimental data, we have identified three different exchange reactions. The first is a rapid intramolecular ring opening/ring closing reaction (hereafter referred to as "ligand rotation") with a time scale approximately 2 orders of magnitude faster than that of the subsequent intermolecular exchange of L and fluoride. The rates of exchange of these reactions are nearly the same but usually larger for fluoride than for L. 4-Nitropicolinate and the proton-catalyzed pathways for carbonate are exceptions. For the latter reaction, we can systematically vary the rate of exchange of carbonate by varying the pH.

Two mechanistic schemes, one describing the exchange reactions in UO_2LF_3 systems and the other for the $UO_2(ox)_2F^{3-}$ complexes, will be used. We will first discuss whether the intermolecular exchange reactions are parallel or consecutive. The fact that the rate of fluoride exchange in general is faster than that of L, but not strongly dependent on the nature of L, suggests two parallel exchange pathways. To corroborate this conclusion, we have determined the rates of reaction and their activation parameters using experimental data over a larger temperature range.

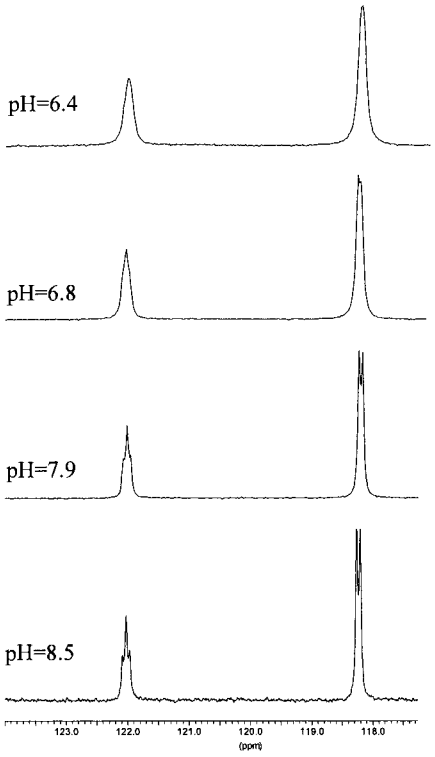

Figure 1. pH dependence of the ^{19}F NMR signals of $UO_2CO_3F_3^{3-}$ (10 mM UO_2^{2+}, 25 mM CO_3^{2-}, and 100 mM fluoride).

Exchange Reactions in the UO_2LF_3 Systems. Carbonate and Fluoride Exchange Reactions in the $UO_2CO_3F_3^{3-}$ Complexes. The ternary dioxouranium(VI)−carbonate−fluoride system will be used as a model because this system allowed a variation of the rate of exchange of L through a proton-catalyzed reaction. The experiments were made in solutions where the dominant species is $UO_2CO_3F_3^{3-}$. The equilibrium hydrogen ion concentration could not be varied much because of dissociation of the complex (Supporting Information, S1). The pseudo first-order rate constant for the carbonate exchange is[2]

$$k(\text{obs}) = k_0 + k_1[H^+] \qquad (2)$$

where $k_0 = 5.7 \pm 2.1$ s^{-1}, and $k_1 = 7.6(0.5) \times 10^8$ M^{-1} s^{-1}. Hence, the carbonate exchange rates are ∼8 and ∼66 s^{-1} respectively at pH = 8.5 and 7.1. ^{19}F NMR magnetization-transfer experiments measured at both pH values showed that the change of the rate of carbonate exchange had no effect on the intermolecular rate of exchange of fluoride, as can be seen in Table 1. This is strong evidence for exchange reactions following two parallel pathways. The increase in the rate of exchange of carbonate resulted in a faster intramolecular site exchange between the coordinated fluorides, as can be seen in the ^{19}F NMR spectra measured at different pH values at −5 °C (Figure 1). The same effect is observed also in the 4-nitropicolinate system, as will be discussed later. On the basis of the temperature dependence of the rate constants which were calculated from the line width of the free fluoride signal, the same activation parameters could be determined for the fluoride exchange at both pH values (Table 1). The Eyring plots are given in Supporting Information, S1.

L and Fluoride Exchange Reactions in the UO_2LF_3 Complexes. Three fluoride peaks, A, B, and C, were observed

(18) *MATLAB for Windows*, 4.2c ed.; Mathworks, Inc.: 1994.
(19) Reeves, L. W.; Shaw, K. N. *Can. J. Chem.* **1970**, *48*, 3641.
(20) *WIN-NMR*, 950901.0 ed.; Bruker-Franzen Analytik GmbH.

Scheme 1. Intra- and Intermolecular Exchange Processes Identified by ^{19}F NMR Spectroscopy for $UO_2(pic)F_3^{2-}$ (pic = Picolinate)

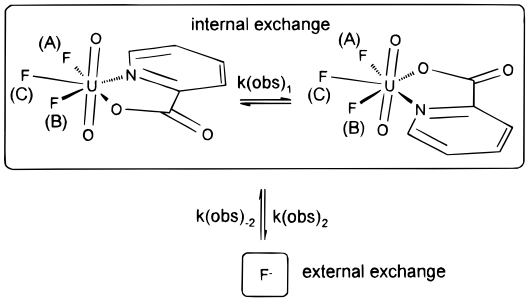

in the ^{19}F NMR spectra of the unsymmetrical UO_2LF_3 complexes (where L denotes picolinate, 4-nitropicolinate, and 4-(3-pentyl)picolinate) because of their different chemical environments (Scheme 1 and Figure 2). Three different coupling constants J_{AB}, J_{AC}, and J_{BC} are expected, with $J_{AC} \approx J_{BC}$. Each fluoride should give rise to a doublet of doublets, where the inner two coalesce to give the observed triplet for the central fluoride. The doublets of doublets for the A- and B-edge fluorides are completely coalesced. The resulting broad signals indicate fast site exchange between them as a result of internal rotation of the picolinate ligand (Scheme 1).

The rates of exchange among the three different fluoride sites and free fluoride at −5 °C for the picolinate system have previously been determined by magnetization-transfer experiments.[2] The rate of the internal rotation is much faster than the longitudinal relaxation rate of the fluorine sites, so the spins of all the fluorines are unchanged during this process. Similar experiments for the 4-(3-pentyl)picolinate and 4-nitropicolinate systems resulted in approximately the same rate constants for the intermolecular fluoride exchange as observed earlier in the other UO_2LF_3 systems at −5 °C, namely, 13.9 ± 1.1 s^{-1} for the edge and 18.2 ± 1.8 s^{-1} for the central fluorides for the 4-(3-pentyl)picolinate and an average value of 16.0 ± 1.2 s^{-1} for the 4-nitropicolinate complex. These values are much lower than the rate constants for the picolinate rotation, which at −5 °C are 90, 300, and 2060 s^{-1} respectively for 4-(3-pentyl)-picolinate, picolinate, and 4-nitropicolinate.

The complete line-shape analyses of the spectra measured at different temperatures allowed us to calculate the exchange rates and the activation parameters for both the intra- and the intermolecular exchange processes for the different picolinate systems. The typical test solution contained 10 mM U(VI), 200 mM fluoride, and 40 mM picolinate at pH = 7.2, where the dominant species are $UO_2(pic)F_3^{2-}$ and free fluoride. First, we calculated the pseudo-first-order rate constants and the activation parameters for the intermolecular fluoride exchange from the line width of the free fluoride signal. Then using the program mentioned in the Experimental Section, we calculated the theoretical line shape of the fluorine peaks at different temperatures. The rates and the activation parameters for the picolinate rotation were determined by a fitting between the measured and calculated spectra (Figure 2). The line broadening of the edge fluoride signals is mainly caused by the fast picolinate rotation in the investigated temperature range; however, the contribution from the intermolecular fluoride exchange had to be taken into account by using the exchange rates calculated previously. The effect of this exchange is clearly seen in the shape of the central fluoride peak, C (Figure 2). The exchange reactions of the 4-(3-pentyl)picolinate complex were studied using the same concentrations as above; however, in the 4-nitropicolinate system, we had to use a picolinate concentration of 100 mM to have a two-site system. This is because the equilibrium constant for the reaction $UO_2^{2+} + L^- + 3F^- \rightleftharpoons UO_2LF_3^{2-}$ is smaller than those for the other picolinate ligands (log β = 13.4 as compared to log β = 14.1 for the picolinate system). The equilibrium constant was calculated from the fluorine integrals at various total fluoride concentrations. The Eyring plots for both the inter- and intramolecular exchanges are shown in the Supporting Information, S2.

The intermolecular picolinate and 4-nitropicolinate exchange could be investigated by ^1H NMR spectroscopy as described before.[2] Line-shape analysis of the signal of the free picolinate was used to determine the rates and activation parameters using the same test solutions as described above. The rate of exchange of the 4-nitropicolinate is much faster than those of the other bidentate ligands in these types of systems (cf. Table 1), with the exception of acetate.[2] The exchange rate is also larger than the coupling (37 Hz) between the coordinated fluorides, which results in an additional "site" exchange between them, as observed by the collapse of the central fluoride "triplet" (Supporting Information, S3). The activation parameters calculated from the temperature dependence of k(obs) are listed in Table 1. For the corresponding oxalate system, the activation parameters for the intermolecular fluoride and oxalate exchange were determined by the line-shape analyses of the free fluoride and the oxalate signals, respectively. The activation parameters for the fluoride exchange also were determined in D_2O, and the experimental results are given in Table 1. (The equilibrium distributions for the investigated solutions and the Eyring plots can be seen in Supporting Information, S4−S6.)

Mechanism for Ligand Rotation Reactions in UO_2LF_3 Complexes. The ligand rotation which is much faster than the intermolecular ligand exchange reactions can only be studied in the picolinate complexes as detailed above. Scheme 2 indicates that the ring opening takes place at the nitrogen end (X) of the coordinated picolinate. The reasons for this assumption are (i) the rate of the ring opening is strongly dependent on the electron density at the coordinated nitrogen atom, as was demonstrated in a previous paper;[2] (ii) the pyridine nitrogen is a much weaker donor than the carboxylate oxygen, as indicated by their stability constants;[14] (iii) the comparatively long U−N bond distance, 2.593(5) Å from a single-crystal structure determination[21] of $Na_2UO_2(pic)F_3 \cdot 3H_2O$, indicates a weak U−N bond; and (iv) a steric repulsion exists between the hydrogen in the 6-position of the pyridine ring and the closely spaced fluoride, as indicated by the large downfield shift in both the proton and the fluorine NMR spectra.

The activation parameters for the ligand rotation in picolinate, 4-(3-pentyl)picolinate, and 4-nitropicolinate are significantly different (cf. Table 1), with the activation entropy for the weakly bonded 4-nitropicolinate much larger than those for the other two ligands. The ligand rotation and the corresponding rate constant are shown in Scheme 1, and the intimate mechanism is indicated in Scheme 2, with two possible pathways for the ring-opening reaction. There is no evidence of the presence of unidentate L at equilibrium, indicating that the equilibrium constant for the ring opening, $K = k_1/k_{-1}$, is smaller than 0.05; hence, the experimental rate constant k(obs) ≈ k_1, and the rate of the ring closure is at least 20 times larger. The two pathways in Scheme 2 differ by the degree of water participation in the transition state. 1 and 2 are the intermediates of D and I_D mechanisms, respectively, and intermediate 1 is expected to have

(21) Aas, W. *Acta Crystallogr., Sect. C*, submitted for publication.

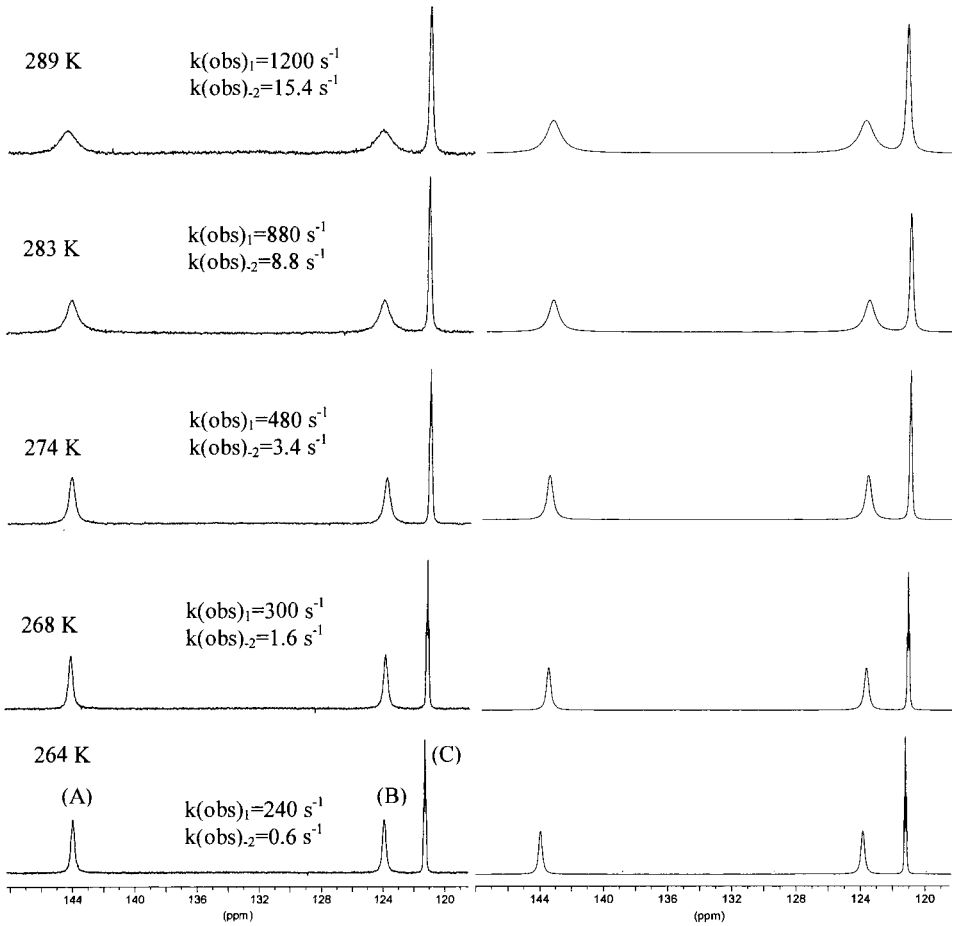

Figure 2. Measured and calculated ^{19}F NMR spectra for the peaks of $UO_2(pic)F_3^{2-}$ (pic = picolinate) at different temperatures (10 mM UO_2^{2+}, 40 mM picolinate, and 200 mM fluoride, pH = 7.2). The calculation of the intra- [$k(obs)_1$] and the intermolecular [$k(obs)_{-2}$] pseudo-first-order rate constants are detailed in the text. The free fluoride signal at around 0 ppm is not shown.

Scheme 2

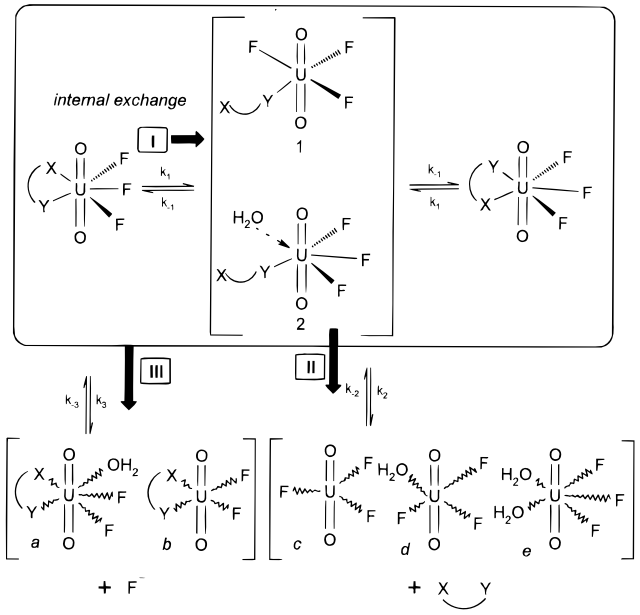

a larger activation entropy than intermediate 2. The experimental activation entropy is much larger for the ring opening in the 4-nitropicolinate complex than for those of the other two picolinate ligands, i.e., the former follows the path to intermediate 1 and the other two follow the path leading to intermediate 2. This suggestion is compatible with the experimental rate constant of water exchange (approximately 1600 s^{-1} in $UO_2(ox)F_2(H_2O)^{2-}$, a model for the intermediate 2), which is larger than k_1 and k_{-1} in the picolinate and 4-(3-pentyl)picolinate complexes but not in the 4-nitropicolinate complex.

Mechanisms for the Intermolecular Exchange Reactions in UO_2LF_3 Complexes. There are two parallel intermolecular exchange reactions in Scheme 2. Because the intramolecular reactions of UO_2LF_3 are much faster than the intermolecular ones, the species within the top square of Scheme 2 are in equilibrium with one another.

A. Fluoride Exchange in UO_2LF_3 Complexes. Path III describes the exchange of fluoride taking place parallel to that of L. The first step is the rate-determining dissociation of fluoride, with or without water mediation in the transition state (a and b in Scheme 2), followed by a fast reentry of fluoride. The rate is equal to

$$v = k_3[UO_2LF_3] \qquad (3)$$

The activation parameters $\Delta H^{\ddagger}$ and $\Delta S^{\ddagger}$ (Table 1) are approximately the same in the different picolinate and oxalate complexes (Supporting Information, S7), indicating that the fluoride bond breaking is not strongly dependent on L. This also is found in the ground state, where the equilibrium constants for the formation of UO_2LF_3 from UO_2LF_2 and F^- are nearly the same for the different oxalate and picolinate complexes.[14]

The activation entropies for the fluoride exchange reactions are all small and positive, indicating that fluoride bond breaking is more important than water bond formation in the transition

state, as expected for an I_D mechanism. The rate constants and the activation parameters are approximately the same in H_2O and D_2O, indicating that there is no large change in solvation of the leaving fluoride (cf. Table 1).

B. L Exchange in UO_2LF_3 Complexes. We have assumed that the carbonate system can be used as a model for all of these systems; i.e., the exchange takes place along the separate pathway II. The activation parameters for the exchange of L are composite quantities (eq 2), and therefore vary much more than those of the fluoride exchange. The exchange is assumed to take place through sequential breaking of the two bonds in L, with varying participation of water in the transition states (1 and 2 and c−e in Scheme 2). The rate-determining step is the breaking of the second bond (the rate constant k_2). Using the steady-state approximation, the rate of exchange of L along II is equal to

$$v = \frac{k_1 k_2}{k_{-1} + k_2}[UO_2LF_3] \cong \frac{k_1 k_2}{k_{-1}}[UO_2LF_3] \qquad (4)$$

The rate expression may be simplified because $k_{-1} \gg k_2$.

The validity of the steady-state approximation can be checked in the picolinate system where $k_1 = 300\ s^{-1}$, $k_1/k_{-1} < 0.05$, and $k_2 < 94\ s^{-1}$; i.e., $k_{-1} > k_1 \gg k_2$. The value of k_1 cannot be determined in the oxalate system, as explained previously. However, the rate should be at least 10 times smaller than that in the picolinate system, because it involves a charge separation (cf. the following discussion of the exchange reactions in the $UO_2(ox)_2F^{3-}$ complexes). At the same time, the oxalate chelate is much more stable than the picolinate chelate; i.e., the ratio $k_1/k_{-1} < 0.001-0.01$. Using these estimates, one finds that the steady-state approximation also is reasonable in the oxalate system. In the 4-nitropicolinate system and the carbonate system at pH = 6.5, the rates of exchange of L are much larger than that of fluoride, indicating the formation of an intermediate/transition UO_2F_3. By varying the concentration of the free carbonate and hydrogen carbonate in the test solutions, we found that the line width of $UO_2F_3(H_2O)_2^-$ was unaffected by the carbonate exchange (cf. Supporting Information, S8 and S9). From this, we can conclude that UO_2F_3 is *not* identical with $UO_2F_3(H_2O)_2^-$ but must contain a lower number of coordinated water molecules. This finding is a clear indication of an intermediate/transition state without water participation, i.e., of a dissociative mechanism for the L exchange.

Exchange in the UO_2L_2F Complexes. Two different isomers for $UO_2(pic)_2F^-$ were previously identified by their proton and fluorine signals at low temperatures in methanol.[2] The exchange between them takes place through a ring opening/ligand rotation/ring closing sequence, and the activation parameters are $\Delta S^{\ddagger} = -82.9 \pm 0.6\ J\ mol^{-1}\ K^{-1}$ (erroneously given as a positive value in our previous paper[2]) and $\Delta H^{\ddagger} = 26.9 \pm 0.5\ kJ\ mol^{-1}$. The solvent effect on the activation parameters for the ligand rotation was investigated by dissolving the solid compound in dimethyl sulfoxide. Separate fluorine signals were observed for the two isomers at room temperature, because of a slower rate of exchange and a much larger chemical shift difference between the fluoride signals. The following very different activation parameters which indicate the strong solvent dependence (between methanol and DMSO) were obtained: $\Delta S^{\ddagger} = -27.8 \pm 2.6\ J\ mol^{-1}\ K^{-1}$ and $\Delta H^{\ddagger} = 45.9 \pm 1.4\ kJ\ mol^{-1}$. For comparison, the calculated exchange rates between the isomers at 25 °C in methanol and dimethyl sulfoxide are 5500 and 2400 s^{-1}, respectively.

The exchange between the isomers is too fast to give separate fluorine signals in water, but the intermolecular fluoride exchange and the corresponding activation parameters (cf. Table 1) could be determined from the line width of the free fluoride signal in a test solution containing 5 mM U(VI), 90 mM picolinate, and 10 mM fluoride.

Scheme 3

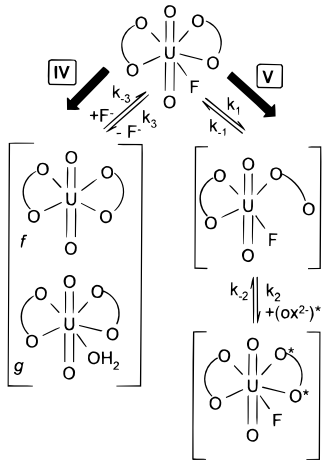

The activation parameters of the two ligand exchange reactions in $UO_2(ox)_2F^{3-}$ were determined as described above. Their values are nearly the same (cf. Table 1), which may indicate that the exchange reactions have a common intermediate (e.g., $UO_2(ox)_2$; cf. Scheme 3). The fluoride exchange was investigated in both H_2O and D_2O (cf. Table 1). (The equilibrium distributions for the investigated solutions and the Eyring plots can be seen in Supporting Information, S10−S12.)

Mechanisms for the Intermolecular Exchange Reactions in UO_2L_2F Complexes. A detailed study of both ligand exchange reactions could only be made for the oxalate system. It was not possible to make a direct study of the "rotation" of the oxalate because the ^{13}C chemical shift differences between the two nonequivalent carbon atoms on the coordinated oxalate ligand are too small. The exchanges of oxalate and fluoride are both first-order reactions, with the rate of exchange of fluoride faster than that of oxalate in the entire temperature range investigated. At −5 °C, the k(obs) values for oxalate and fluoride are 8.7(1.5) and 12.3(1.0) s^{-1}, and at 55 °C, they are 132 and 316 s^{-1}, respectively. The activation parameters for both reactions are nearly the same, and the possible mechanisms for the exchange reactions are given in Scheme 3. We suggest that the exchange reactions for this complex also follow two parallel pathways. The rate-determining step along path V is the opening of the oxalate chelate ring [k(obs) = 8.7 $s^{-1} \approx k_1$], followed by a fast exchange with free oxalate and ring closure. The faster fluoride exchange cannot take place after the ring opening along this pathway. The first step along path IV is the dissociation of fluoride [k(obs) = 12.3 s^{-1}]. The exchange of oxalate then may take place as a consecutive reaction along this path, provided that the rate of the chelate ring opening is slower than the subsequent oxalate exchange steps. In this case, we cannot use the steady-state approximation to obtain a relationship between k(obs) for the oxalate exchange and the rate constants in the proposed mechanism. Both of the mechanistic pictures discussed above are consistent with the experimental observations; however, we prefer the model with exchange along two parallel pathways. The mechanism is analogous to the one discussed by Fukutomi et al.[5] and Delpuech et al.[8]

The activation parameters for the fluoride exchange in $UO_2(ox)_2F^{3-}$ vary between H_2O and D_2O, indicating solvent

Table 2. Rate Constants at −5 °C for Different Proton-Catalyzed Exchange Processes

reaction	k_0 (s^{-1})	k_1 (M^{-1} s^{-1})	k_2 (M^{-1} s^{-1})	k_3 (M^{-1} s^{-1})
$UO_2(ox)_2F^{3-} \leftrightarrows$ ox	5.7(1.0)	$7.5(0.6) \times 10^3$	$2.5(0.2) \times 10^2$	
(in D_2O)	8.3(1.0)	$1.1(0.1) \times 10^4$		
$UO_2(ox)F_3^{3-} \leftrightarrows$ ox	4.6(1.3)	$1.9(0.2) \times 10^4$	$8.2(2.0) \times 10^1$	
$UO_2(ox)_2F^{3-} \leftrightarrows F^-$	14.2(1.6)	$2.0(0.5) \times 10^4$	$2.8(1.1) \times 10^2$	$3.5(1.5) \times 10^1$
(in D_2O)	13.8(1.5)	$4.2(0.2) \times 10^4$		
$UO_2(ox)F_3^{3-} \leftrightarrows F^-$ [a]	18.1(3.2)	$6.8(1.0) \times 10^4$	$6.1(2.2) \times 10^2$	$1.4(0.4) \times 10^2$
(in D_2O)	19.5(1.5)	$1.2(0.1) \times 10^5$		
$UO_2(ox)F_3^{3-} \leftrightarrows F^-$ [b]	13.2(2.1)	$4.1(0.6) \times 10^4$	$4.0(1.4) \times 10^2$	$1.0(0.4) \times 10^2$
(in D_2O)	12.6(1.2)	$8.1(0.1) \times 10^4$		

[a] For the central. [b] For the edge fluorides.

participation in the transition state. The activation entropy, $\Delta S^{\ddagger}$, for the fluoride exchange in UO_2L_2F systems is much more negative than those of the corresponding UO_2LF_3 complexes. Both of these observations indicate an increased solvation (through the formation of strong hydrogen bonds) of the leaving fluoride in the transition state, where it is more exposed to the solvent, than in the ground state. This difference is much smaller in the UO_2LF_3 complexes.

Proton- and Acid-Catalyzed Exchange Pathways. In the previous paper,[2] we described how proton catalysis may be used to deduce mechanistic information. In this paper, we also have used deuterium substitutions to obtain additional information of this type. The pH dependence of the rates of the fluoride and oxalate exchange reactions was investigated by using test solutions in which the total concentrations were selected in such a way that the concentrations in the solutions of $UO_2(ox)_2F^{3-}$ and $UO_2(ox)F_3^{3-}$ were not changed appreciably when the hydrogen ion concentration was varied between pH = 3 and 7 (typical diagrams are shown in Supporting Information, S13). The pseudo-first-order rate constants for the fluoride exchange depend on the hydrogen ion concentration at different total fluoride and acetate concentrations. The weakly coordinated acetic acid (Hac) was studied in order to have an acid catalyst which does not participate in the exchange reaction. The total fluoride concentration was varied to change the equilibrium HF concentration at a given pH in order to observe if this affects the rate or not. The observed rate constants for the proton- and acid-catalyzed fluoride pathways are

$$k(\text{obs}) = k_0 + k_1[H^+] + k_2[HF] + k_3[\text{Hac}] \qquad (5)$$

The experimental values of k_i ($i = 1-3$) are given in Table 2 and are all based on magnetization-transfer experiments (see the Experimental Section). The different curves (shown as Supporting Information, S14a) have been calculated from these rate constants.

Experiments repeated in D_2O show that the effects of DF and Dac are much smaller and the rate constants k_2 and k_3 cannot be determined in the deuterium system (Supporting Information, S14b). However, there is a large reverse-isotope effect for the proton-catalyzed exchange, and k_1 is approximately twice as large in D_2O as it is in H_2O.

The pH dependence of the oxalate exchange rates for the same complexes was investigated by ^{13}C NMR inversion-transfer experiments at different total concentrations of HF and Hac. (The results in H_2O for $UO_2(ox)_2F^{3-}$ are shown in Supporting Information, S15.) The curves have been calculated using the rate constants given in Table 2. The proton-catalyzed exchange (k_1) is approximately 1.5 times larger in D_2O than that of H_2O. There is no measurable catalytic effect of acetic acid on the oxalate exchange, and the catalytic effect of HF also is small. The effect of DF (k_3) cannot be measured.

Mechanism for the Proton-Catalyzed Exchange Reactions. In the ternary systems, the proton-catalyzed reaction is the predominant pathway for the exchange of carbonate, oxalate, and fluoride at low pH. The most important of the catalyzed reactions are the ones involving protons; the HF- and Hac-catalyzed reactions are much slower.

The experiments in H_2O and D_2O showed a pronounced reverse-isotope effect for the proton catalyzed pathways but normal isotope effects for the HF- and Hac-catalyzed pathways. The rate constants for the noncatalyzed pathway (k_0) are identical within the experimental error in both solvents. The faster exchange of fluoride in D_2O may be a kinetic isotope effect or the result of a preequilibrium involving the binding of H^+/D^+ to a coordinated fluoride; i.e., the rate constant k_1 is a product of an equilibrium constant and a rate constant, where the equilibrium constant is larger for the bonding of D^+ than that of H^+. We prefer the second explanation, and this was used to describe the proton catalysis in the binary uranyl-fluoride[1] and carbonate systems.[22] The normal isotope effect for HF and Hac indicates that they act as proton donors which are not directly involved in the reaction.

A comparison between the HF pathways in the binary and ternary systems indicates that the fluoride exchange follows different mechanisms. In the former system, the fluoride exchange involves a concerted bonding of the HF/DF to uranium and an "internal" proton transfer from the entering HF/DF to the leaving F^- (or water). In the ternary complexes, HF/DF acts as H^+/D^+ donors in a preequilibrium in which the fluoride in HF/DF does not interact with uranium.

Conclusions

The rates for the intermolecular ligand exchange in the UO_2LF_3 and UO_2L_2F complexes depend only on the concentration of the complex, and the reactions take place along parallel pathways. In UO_2LF_3, the activation entropies for the fluoride exchange have small positive values which are nearly the same in H_2O and D_2O, indicating an I_D intimate mechanism. The complete mechanism for the exchange of L could only be studied for the unsymmetrical picolinate ligands, but we assume that the symmetric ligands follow the same mechanistic pattern. The exchange proceeds in two steps, where the first is a fast intramolecular ring opening/ring closing (denoted as ligand rotation) and the second is a slower bond breaking at the carboxylate end of the ligand. The rates and activation entropies for the ring-opening reactions vary strongly with the substituents on the picolinate ligand, indicating different degrees of water participation in this step. The ligand rotation in 4-nitropicolinate is so fast that hydration in its transition state is less likely than

(22) Bányai, I.; Glaser, J.; Micskei, K.; Tóth, I.; Zékány, L. *Inorg. Chem.* **1995**, *34*, 3785.

hydration in the 4-(3-pentyl)picolinate system, where this step is much slower.

The rate-determining step for the oxalate exchange in $UO_2(ox)_2F^{3-}$ is the opening of the oxalate ring. The rate constant ($\sim$9 s^{-1}) is much lower than that for the picolinate in the UO_2LF_3 systems, which varied from 90 to 2060 s^{-1}, depending on the substituent on the ligand. The activation entropies for the exchange of fluoride in $UO_2(ox)_2F^{3-}$ have large negative values with a pronounced H/D isotope effect. This indicates a significant change in the solvation of the leaving fluoride between the initial and the activated states.

Acknowledgment. We are grateful to Franz Georg och Gull Liljenroth's Stiftelse for a research fellowship covering Z.S.'s stay in Stockholm and to the Swedish Nuclear Fuel and Waste Management Co. (SKB) for their financial support.

Supporting Information Available: Various equilibrium ligand distribution diagrams as a function of pH and Eyring plots of the temperature dependence of the rate constant for exchange between the complexes and free ligand (S1, S4−S7, and S10−S12); equilibrium distribution diagrams and Eyring plots of inter- and intramolecular fluoride exchange rate constants for $UO_2(pic)F_3^{2-}$ (S2); ^{19}F NMR spectra for UO_2LF_3 complexes, where L = 4-nitropicolinate and picolinate (S3); equilibrium uranium and carbonate distribution diagrams and ^{19}F NMR spectra of solutions at various total fluoride concentrations (S8 and S9); examples of equilibrium fluorine and oxalate distribution diagrams as a function of pH which were used for solutions during investigations of the proton-catalyzed exchange processes (S13); pH dependence of the pseudo-first-order rate constants of various complexes for fluoride (S14) and oxalate (S15) exchange reactions (15 pages). Ordering information is given on any current masthead page.

IC9804364